

Dephasing Time in Disordered Systems

C. Castellani

Dipartimento di Fisica, Università dell'Aquila, Aquila, Italy, and Dipartimento di Fisica, Università "La Sapienza," Roma, Italy, and Gruppo Nazionale di Struttura della Materia, Unità dell'Aquila, Aquila, Italy

C. DiCastro

Dipartimento di Fisica, Università "La Sapienza," Roma, Italy, and Gruppo Nazionale di Struttura della Materia, Unità di Roma, Roma, Italy

and

G. Kotliar and P. A. Lee

Department of Physics, Massachusetts Institute of Technology, Cambridge, Massachusetts 02139

(Received 12 November 1985)

We show that interaction effects give rise to a cutoff $1/\tau_{ph}$ in the "diffusion," the basic propagator of the disordered interacting electron gas. We calculate $1/\tau_{ph}$ to lowest order in the disorder but to all orders in the interaction, and exhibit its relation to the scaling variables of the disordered-interacting-electron problem. This framework provides an explanation for the anomalous enhancement of inelastic processes which is observed experimentally in systems close to the metal-insulator transition.

PACS numbers: 71.55.Jv, 71.30.+h

The quasiparticle inelastic lifetime, τ_{in} , is a central quantity in localization theory. It sets the scale over which an electron propagates without undergoing inelastic scattering, via the Thouless¹ relation $l_{in}^2(T) = D\tau_{in}(T)$, and has been studied experimentally in magnetoresistance measurements.² Since the origin of inelastic scattering is the diffusion-enhanced Coulomb interaction, it is important to incorporate this quantity into the more general framework of a theory including localization and interactions. The first calculation of $\tau_{in}(T)$, due to Schmid,³ revealed that disorder increases the inelastic rate leading to $1/\tau_{in}(T) \sim T^{d/2}$ which is, at low temperatures, much larger than the Landau Fermi-liquid theory expression $1/\tau_{in}(T) \sim T^2$. Later, Fukuyama and Abrahams⁴ identified $1/\tau_{in}(T)$ with $1/\tau_{pp}$, the mass of the Cooperon, i.e., the diffusive propagator in the particle-particle channel. Several mechanisms of inelastic scattering⁵⁻⁸ have been considered. These are reviewed by Abrahams.⁹

In this Letter we show that inelastic effects provide a cutoff $1/\tau_{ph}$ to the "diffusion," i.e., the diffusive propagator in the particle-hole channel. This result can be shown to be consistent with particle and spin conservation. In the framework of the existing scaling theory of localization and interactions, the inelastic rate increases very fast as we move to larger scales, suggesting that inelastic effects are dominant close to the metal-insulator transition. In particular, interaction-induced divergences might be cutoff by $1/\tau_{ph}(T)$ and not by the temperature as is usually assumed.^{10,11}

We study the dephasing time in the framework of the scaling theory of interacting disordered fermions

using the formulation of Castellani *et al.*¹² We define the scaling variables of this theory and summarize the relevant notation below. The diffusion propagator, L , is defined by the sum of graphs describing electron-hole propagation *without energy exchange* between the electron and hole line. To lowest order in the disorder and in the absence of interactions, it is given by L_0 , which sums the graphs in Fig. 1. Interaction effects result in a self-energy correction Σ . At zero temperature¹² the self-energy correction results in a modification of the bare diffusion constant, a rescaling of the frequency by a factor Z , and an overall rescaling of the diffusion propagator by a factor ξ^2 . The new feature to be discussed in this Letter is that at finite temperatures $\Sigma(\Omega = 0, q = 0)$ no longer vanishes and it gives rise to the diffusion inelastic lifetime $1/\tau_{ph}$:

$$L(q, \Omega) = \frac{1}{L_0^{-1} - \Sigma} = \frac{\xi^2}{Dq^2 + Z\Omega + 1/\tau_{ph}}. \quad (1)$$

The variable ξ is the ratio of the renormalized density

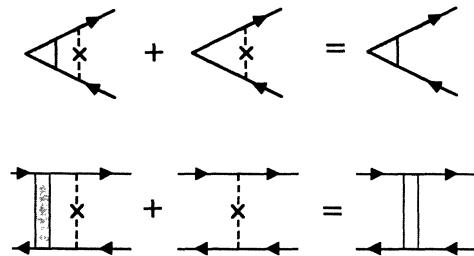


FIG. 1. Bare diffusion and diffusive vertex.

of states to the bare density of states N_0 .¹³ The other scaling variables are defined in terms of the static amplitudes: $\tilde{\Gamma}_1$ and $\tilde{\Gamma}_2$ denote the Hartree and Fock static scattering amplitudes. They are related to the singlet and triplet scattering amplitudes via $\tilde{\Gamma}_s = \tilde{\Gamma}_1 - \frac{1}{2}\tilde{\Gamma}_2$, $\tilde{\Gamma}_t = -\frac{1}{2}\tilde{\Gamma}_2$.

The scaling variables Γ_1 and Γ_2 are defined by $\Gamma_1 = \xi^2 \tilde{\Gamma}_1$, $\Gamma_2 = \xi^2 \tilde{\Gamma}_2$. This definition eliminates ξ from the scaling equations.¹² The self-energy graphs of lowest order in the scaling variable $t = 1/(2\pi)^2 N_0 D$ are shown in Fig. 2. The calculation is done to lowest order in t but to all orders in the interaction. Therefore the wavy lines in Fig. 2 will be expressed in terms of the dynamical amplitudes (ladder resummations of static amplitudes and diffusions) defined as

$$\tilde{U}_s(q, \omega) = \left\{ \tilde{\Gamma}_2 - \frac{\tilde{\Gamma}_2}{2} \right\} \frac{Dq^2 + Z|\omega|}{(Dq^2)}, \quad \tilde{U}_2(q, \omega) = \tilde{\Gamma}_2 \frac{Dq^2 + Z|\omega|}{Dq^2 + Z_2|\omega|}.$$

We use the notation $Z_2 = Z + \Gamma_2$.

At zero temperature the graphs in Fig. 2 are proportional to Ω , the external frequency, and q^2 , the external momenta. We evaluate these diagrams at finite temperature T , using the Matsubara technique. The only part which is not manifestly proportional to Ω and q^2 originates in Figs. 2(d) and 2(h) and is given by

$$\Sigma' = \frac{T}{N_0} \sum_{\epsilon_n < \omega_1 < \epsilon_n + \Omega} \int \frac{d^d k}{(2\pi)^d} [U_s(k, \omega_1) - \frac{3}{2}U_2(k, \omega_1)] \frac{1}{Dk^2 + Z|\omega_1 + \Omega|}.$$

Note that the sum over the Matsubara frequencies ω_1 in the expression for Σ' is restricted. Nevertheless, it is not correct to conclude that Σ' is proportional to Ω . The sum on ω_1 crosses zero, a point where the summand is not analytic. The sum must be evaluated along the lines of Ref. 4, using the analytic continuation technique which gives rise to a contribution from a branch cut which does not vanish as the external frequency and momenta go to zero:

$$\Sigma(0, 0) = \frac{2}{\pi N_0} \int_{-\infty}^{\infty} \frac{dx}{\sinh \beta x} \int \frac{d^d p}{(2\pi)^d} L_R(p, x) \text{Im} \{ \tilde{U}_s(x) - \frac{3}{2}\tilde{U}_2(x) \}_R. \tag{2}$$

The subscript R indicates that a replacement $|\omega| \rightarrow -ix$ is performed to obtain the retarded part of these functions.

The presence of a mass in the particle-hole channel seems, at first sight, to contradict particle conservation. The density-density polarization function has the skeleton structure shown in Fig. 3(a). In the presence of long-range forces one separates the singlet amplitude $\tilde{\Gamma}_s$ into a short-range part and a long-range part. Only the short-range part $\tilde{\Gamma}_s^{sr}$ enters π which is irreducible with respect to the long-range Coulomb force. Figure 3(a) corresponds to the following expression:

$$\pi(q, \Omega) = \frac{dn}{d\mu} - \frac{2N_0 K^2 \Omega}{L^{-1} - \sum_{\epsilon_n < \omega_1 < \epsilon_n + \Omega} 2\tilde{\Gamma}_s^{sr}}. \tag{3a}$$

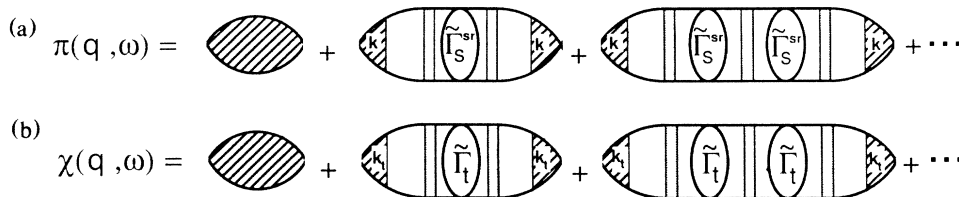


FIG. 3. (a) Skeleton structure of the density-density correlation. (b) Skeleton structure of the spin susceptibility.

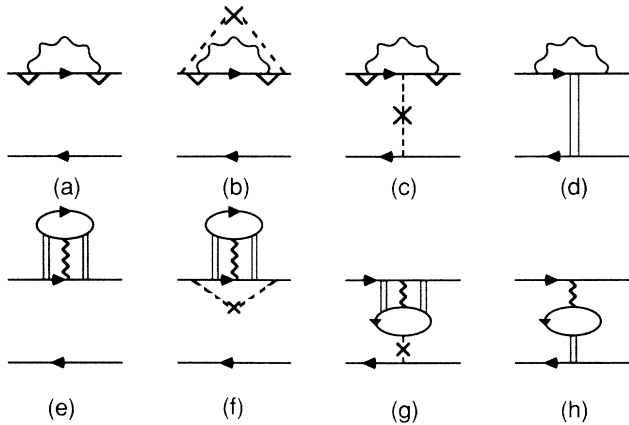


FIG. 2. Self-energy diagrams to lowest order in t .

The first diagram in Fig. 3(a) is $dn/d\mu$, and K is the charge vertex at zero frequency. The presence of a mass term in the denominator of the second term of Eq. (3a) apparently makes it impossible to satisfy the condition $\pi(q=0, \Omega)=0$ which follows on very general grounds from particle conservation. We show that this is not the case; $\Sigma(0,0)$ is canceled in $\pi(q, \Omega)$ by the corrections to $\tilde{\Gamma}_s^{sr}$.

The perturbative evaluation of the correction to the amplitudes (see Fig. 4) contain terms which cross a point of nonanalyticity as the sum in Eq. (3a) is performed. Only graphs of the lowest order in the dynamical amplitude [i.e., graphs (a) and (b) in Fig. 4] eliminate $1/\tau_{ph}$ from the density-density correlator. In fact, the contribution of nonanalytic pieces of graphs 4(c)–4(f) to Eq. (3a) cancel among themselves. Inserting the expressions for the graphs depicted in Figs. 4(a) and 4(b) and doing the Matsubara sums by standard techniques, we find branch-cut contributions which exactly cancel $1/\tau_{ph}$ and restore particle conservation. This cancellation, which takes place to all orders in the interaction strength, is a strong check on the validity of the renormalization scheme for the interacting-electron problem.

Similar considerations apply to the spin-spin correlation function. Its skeleton decomposition, shown in Fig. 3(b), and discussed in detail in Ref. 13, can be summarized in

$$\chi(q, \Omega) = \chi_{st} - \frac{2N_0 K_t^2 \Omega}{L^{-1} - 2N_0 \sum_{\epsilon_n < \omega_1 < \epsilon_n + \Omega} \tilde{\Gamma}_t}. \quad (3b)$$

χ_{st} is the static susceptibility, and K_t the triplet spin vertex at zero frequency.

The mass in the triplet channel is canceled by a contribution from the Matsubara sum in Eq. (3b) which does not vanish as $\Omega \rightarrow 0$. The cancellation in the triplet channel is slightly different from its singlet counterpart. Graphs 4(b), 4(e), and 4(f) do not contribute to Eq. (3b) since they only renormalize $\tilde{\Gamma}_1$ and

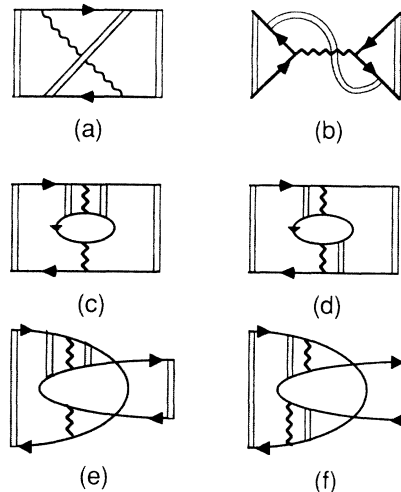


FIG. 4. Scattering-amplitude renormalizations.

$1/\tau_{ph}$ in Eq. (3b) is canceled by graphs 4(a), 4(c), and 4(d).

We note that Eq. (2) contains a logarithmic divergence in two dimensions. However, this divergence is very different in nature from that of the other scaling variables of the interacting-electron problem, D , Z , and Γ_2 .¹⁴ Perturbative evaluation of these quantities reveal that they are ultraviolet divergent; all momenta within the region $T \leqq Dq^2 \leqq 1/\tau$ where the Wilson rescaling procedure is applied make equal contributions to their renormalization. $1/\tau_{ph}$, on the other hand, does not contain new ultraviolet divergences. The scale dependence of $1/\tau_{ph}$ arises from the scale dependence of D , Z , and $Z_2 = Z + \Gamma_2$. It is infrared divergent because momentum scales $0 \leqq Dq^2 \leqq T$ make an equal contribution to the integral. This divergence is not cured by the renormalization group. A lower cutoff has to be introduced by a self-consistency requirement. As pointed out by Fukuyama,¹⁵ $1/\tau_{ph}$ enters physical quantities at finite momentum scale $Dq^2 \sim 1/\tau_{ph}$ and we will use this as our lower cutoff in Eq. (2). Evaluating Eq. (2) with this prescription we obtain an expression for $1/\tau_{ph} = \zeta^2 \Sigma(0,0)$:

$$\frac{1}{T\tau_{ph}} = 4t \int_{1/(\tau_{ph}T)}^{\infty} \frac{d\lambda}{\lambda} \left[\Gamma_s \arctan \frac{Z}{\lambda} + \frac{3}{2(Z_2 + Z)} \right] \Gamma_2 \left[\frac{Z_2}{\lambda} \arctan \frac{Z_2}{\lambda} - \frac{Z}{\lambda} \arctan \frac{Z}{\lambda} \right]. \quad (4)$$

This expression is valid to lowest order in t but to all orders in the interaction amplitudes.

In the weakly localized regime, we can ignore the scale dependence of t , Γ_2 , and Z , to solve Eq. (4) for $1/\tau_{ph}$:

$$\frac{1}{T\tau_{ph}} = 2\pi t \left[\Gamma_s \frac{3}{2(Z_2 + Z)} \Gamma_2^2 \right] \ln \frac{1}{t \{ \Gamma_s + [3/2(Z_2 + Z)] \Gamma_2^2 \}}, \quad T\tau_{ph} \gg 1, \quad (5)$$

$$\frac{1}{T\tau_{ph}} \cong [4t(Z\Gamma_s + \frac{3}{2}\Gamma_2^2)]^{1/2}, \quad T\tau_{ph} \cong 1.$$

For strong disorder, the scale dependence of Z_2 , t , and Z is important. These scaling variables flow to strong coupling and the critical behavior of the interacting-electron problem is not fully understood.^{16,17} Nevertheless we can use Eq. (4) to make qualitative statements about $T\tau_{ph}$.

In the framework of the scaling theory of the interacting-disordered-electron problem the scaling variables Z_2 and Γ_2 grow much faster than Z as we scale to longer distances. Therefore, even if $1/\tau_{ph} \ll T$ at the Fermi-liquid level, i.e., before scaling is applied, renormalization effects cause $1/\tau_{ph}$ to grow, suggesting that inelastic effects are important close to the metal-insulator transition. It is, therefore, very likely that the divergences which arise as a result of interactions are cut off by $1/\tau_{ph}$ and not by T as has been done so far.

In the pure localization problem without time-reversal symmetry (the unitary case), the particle-particle channel is suppressed and the logarithmic singularity in the conductivity is driven by the particle-hole channel. The presence of $1/\tau_{ph}$ in the particle-hole channel is then consistent with the physical expectation that inelastic scattering will cut off the logarithmic singularity even in this case. Since the logarithmic divergence in the unitary case is higher order in $(k_F l)^{-1}$ it is usually dominated by interaction effects and has not yet been observed. The only possible exception to this may be the case of short-range interactions,¹² which may be produced in a thin film with external screening provided by a nearby metallic sheet.

In the present framework the particle-hole lifetime, $1/\tau_{ph}$, is identical to the particle-particle propagator lifetime $1/\tau_{pp}$. In fact, by reversing an electron line in the Fock diagrams in Fig. 2 we recover the diagrams of Fukuyama and Abrahams.⁴ The role of $1/\tau_{pp}$ as a pair breaker has been discussed extensively.⁸ Our calculation provides some theoretical justification for the anomalously enhanced pair breaking observed in samples whose normal state is close to the metal-insulator transition.^{18,19}

Finally we note that τ_{pp}^{-1} is measured in magnetoresistance experiments.²⁰ Expression (5), which is correct to lowest order in the disorder but to all orders in the interaction static amplitudes, should be used in the analysis of the experimental data to extract a combination of the interaction amplitudes. We suggest

combining of this data with measurements of the temperature dependence of the conductivity and the magnitude of magnetoresistance which determine different combinations of amplitudes to test the consistency of the scaling theory of the metal-insulator transition.

We would like to acknowledge the hospitality of the Aspen Center for Physics, where part of this research was carried out, and the participants of the Aspen workshop on heavy fermions for many stimulating discussions.

¹D. J. Thouless, Phys. Rev. Lett. **39**, 1167 (1977).

²G. Bergmann, Z. Phys. B **48**, 5 (1982).

³A. Schmid, Z. Phys. **271**, 251 (1974).

⁴H. Fukuyama and E. Abrahams, Phys. Rev. B **27**, 5976 (1983).

⁵A. Schmid, Z. Phys. **259**, 421 (1973).

⁶B. L. Al'tshuler, A. G. Aronov, and D. E. Khmel'nitzkii, Zh. Eksp. Teor. Fiz. **77**, 2028 (1979) [Sov. Phys. JETP **50**, 968 (1979)], and J. Phys. C **15**, 7367 (1982).

⁷M. C. Chang and E. Abrahams, Phys. Rev. B **32**, 1315 (1985).

⁸W. Brenig, M. C. Chang, E. Abrahams, and P. Wölfle, Phys. Rev. B **31**, 7001 (1985).

⁹E. Abrahams, in *Localization and Metal-Insulator Transitions*, edited by H. Fritzsche and D. Adler (Plenum, New York, 1985).

¹⁰B. L. Al'tshuler, A. G. Aronov, D. E. Khmel'nitzkii, and A. I. Larkin, in *Quantum Theory of Solids*, edited by I. M. Lifshits (Izdatel'stvo Mir, Moscow, U.S.S.R., 1982).

¹¹P. A. Lee and T. V. Ramakrishnan, Rev. Mod. Phys. **57**, 287 (1985).

¹²C. Castellani, C. DiCastro, P. A. Lee, and M. Ma, Phys. Rev. B **30**, 527 (1984).

¹³C. Castellani, C. DiCastro, P. A. Lee, M. Ma, J. Sorella, and E. Tabet, to be published.

¹⁴A. M. Finkelstein, Zh. Eksp. Teor. Fiz. **84**, 166 (1983) [Sov. Phys. JETP **57**, 97 (1983)].

¹⁵H. Fukuyama, J. Phys. Soc. Jpn. **53**, 3299 (1984).

¹⁶A. M. Finkelstein, Z. Phys. B **56**, 189 (1984).

¹⁷C. Castellani, C. DiCastro, P. A. Lee, M. Ma, S. Sorella, and E. Tabet, Phys. Rev. B **30**, 1596 (1984).

¹⁸A. F. Hebard and M. A. Paalanen, Phys. Rev. B **30**, 7 (1984).

¹⁹R. C. Dynes, J. P. Garno, G. B. Hertel, and T. P. Orlando, Phys. Rev. Lett. **53**, 2437 (1984).

²⁰D. J. Bishop, R. C. Dynes, and D. C. Tsui, Phys. Rev. B **26**, 773 (1982).

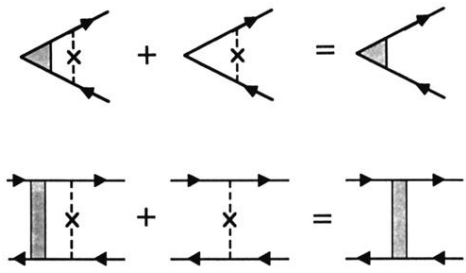


FIG. 1. Bare diffusion and diffusive vertex.

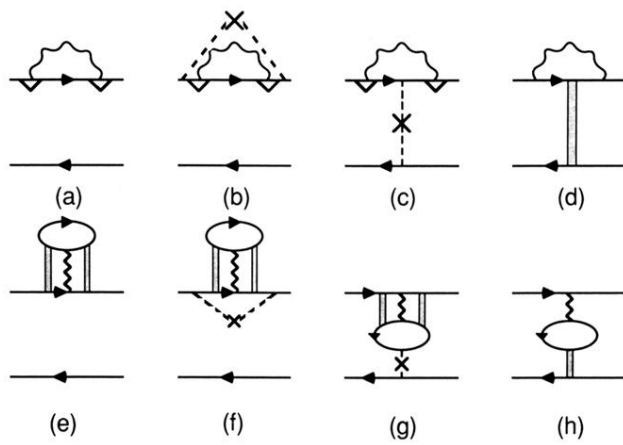


FIG. 2. Self-energy diagrams to lowest order in t .

$$\begin{aligned}
 \text{(a)} \quad \pi(\mathbf{q}, \omega) &= \text{diagram 1} + \text{diagram 2} + \text{diagram 3} + \dots \\
 \text{(b)} \quad \chi(\mathbf{q}, \omega) &= \text{diagram 1} + \text{diagram 2} + \text{diagram 3} + \dots
 \end{aligned}$$

The diagrams are represented as follows:

- Diagram 1:** A shaded oval representing a bare propagator.
- Diagram 2:** A diagram with a central oval labeled $\tilde{\Gamma}_S$ (for (a)) or $\tilde{\Gamma}_t$ (for (b)), flanked by two shaded ovals labeled k .
- Diagram 3:** A diagram with two central ovals labeled $\tilde{\Gamma}_S$ (for (a)) or $\tilde{\Gamma}_t$ (for (b)), flanked by two shaded ovals labeled k .

FIG. 3. (a) Skeleton structure of the density-density correlation. (b) Skeleton structure of the spin susceptibility.